LINC00184 promotes esophageal squamous cell carcinoma progression via DNMT1-mediated methylation of the NDRG2 promoter and PI3K/AKT pathway activation

JUNJUN GUO[1,2*], SHENBO FU[3*], JIA LIU[4], LINA LI[5], JIN ZHAO[3], FENGGANG WANG[3], WENAN WU[3], XU CHEN[5] and ENXIAO LI[2]

[1]Department of Oncology, Shaanxi Provincial Tumor Hospital, Xi'an, Shaanxi 710061, P.R. China;
[2]Department of Oncology, The First Affiliated Hospital of Xi'an Jiaotong University, Xi'an, Shaanxi 710061, P.R. China;
[3]Department of Radiation Oncology, Shaanxi Provincial Tumor Hospital, Xi'an, Shaanxi 710061, P.R. China;
[4]Department of Thoracic Surgery, Shaanxi Provincial Tumor Hospital, Xi'an, Shaanxi 710061, P.R. China;
[5]Department of Internal Medicine, Shaanxi Provincial Tumor Hospital, Xi'an, Shaanxi 710061, P.R. China

Received October 11, 2025; Accepted April 1, 2026

DOI: 10.3892/ol.2026.15628

Abstract. Esophageal squamous cell carcinoma (ESCC) is a highly aggressive cancer with poor clinical outcomes, highlighting the need for enhanced understanding of its molecular drivers. The present study investigated the functional role of long non-coding RNA LINC00184 in ESCC progression. Using overexpression experiments in KYSE-150 and TE-1 cell lines, the present study demonstrated that LINC00184 significantly enhances ESCC cell proliferation and migration while inhibiting apoptosis. Mechanistic studies revealed that LINC00184 recruits DNA methyltransferase 1 (DNMT1) to the promoter of the tumor suppressor gene N-Myc downstream regulated gene 2 (NDRG2), thereby catalyzing CpG island hypermethylation and transcriptional silencing of NDRG2. The subsequent downregulation of NDRG2 results in activation of the oncogenic PI3K/AKT signaling pathway. Notably, treatment with the DNMT1 inhibitor 5-azacytidine reverses LINC00184-induced NDRG2 promoter methylation, restores NDRG2 expression and attenuates PI3K/AKT pathway activation. The present study findings identified a novel LINC00184/DNMT1/NDRG2/PI3K-AKT regulatory axis in ESCC and suggested that targeting this epigenetic pathway may represent a promising therapeutic strategy in the future.

Correspondence to: Professor Enxiao Li, Department of Oncology, The First Affiliated Hospital of Xi'an Jiaotong University, 277 West Yanta Road, Xi'an, Shaanxi 710061, P.R. China
E-mail: oulv309@163.com

*Contributed equally

Key words: LINC00184, esophageal squamous cell carcinoma, N-Myc downstream regulated gene 2, DNA methyltransferase 1, AKT

Introduction

Esophageal squamous cell carcinoma (ESCC) continues to impose a disproportionate global disease burden, with incidence-to-mortality ratios approaching unity and 5-year survival rates remaining <20% (1). Contemporary therapeutic advances, including neoadjuvant chemoradiotherapy and immune-checkpoint blockade, have not markedly improved long-term outcomes. This is largely due to late-stage presentation, early micrometastatic dissemination and primary or acquired therapeutic refractoriness (2). At the molecular level, ESCC exhibits a complex landscape dominated by tumor protein 53 mutations, cell-cycle dysregulation and extensive epigenetic rewiring that collectively orchestrate initiation, invasion and metastatic colonization (3,4). Within this epigenetic circuitry, dysregulation of long non-coding RNAs (lncRNAs) has emerged as a key driver that modulates chromatin architecture, transcriptional programs and post-transcriptional networks, thereby offering tractable biomarkers and therapeutic vulnerabilities for precision oncology (5).

lncRNAs are >200 nucleotides in length and lack canonical open reading frames, yet they exert pleiotropic regulatory functions by sculpting chromatin topology, orchestrating transcription factor assemblies and modulating mRNA stability and translation efficiency (6-8). Among these transcripts, LINC00184 has been repeatedly implicated in oncogenesis, serving as an independent predictor of poor prognosis in breast cancer (9) and associating with aggressive disease courses in gastric cancer through its ability to accelerate G_1/S transition and metastatic dissemination (10). Nevertheless, its functional contribution to ESCC and the molecular circuits it governs remain to be elucidated.

CpG dinucleotide methylation, installed and maintained by DNA methyltransferases (DNMT), constitutes a principal epigenetic switch that silences gene expression through the addition of methyl moieties to promoter-rich CpG islands (11). Hypermethylation of tumor-suppressor loci is a universal

hallmark of malignancy (12). As the principal maintenance DNA methyltransferase, DNA methyltransferase 1 (DNMT1) perpetuates pre-existing methylation marks through successive cell divisions, thereby locking tumor-suppressor genes in a long-term silent state. Consistent with this function, DNMT1 is frequently upregulated across diverse cancer types, including prostate, pancreatic and gastric cancer, and serves a key role in extinguishing anti-oncogenic transcriptional programs (13-15). This epigenetic silencing mechanism is exemplified in ESCC by the tumor suppressor N-Myc downstream regulated gene 2 (NDRG2). While NDRG2 is established to inhibit proliferation and promote apoptosis in various cancer types, including lung, liver and pancreatic cancer (16-18), its expression is consistently downregulated in ESCC, a phenomenon strongly associated with promoter hypermethylation (19,20). Notably, NDRG2 functions as a key upstream inhibitor of the oncogenic PI3K/AKT pathway; NDRG2 can suppress pathway activity by enhancing PTEN or recruiting protein phosphatase 2A (PP2A) to facilitate AKT dephosphorylation, thereby curbing tumor growth (21). Since hyperactivation of the PI3K/AKT axis is a major driver of ESCC progression (22), the epigenetic silencing of NDRG2 presents a plausible mechanism for its constitutive activation. lncRNAs have emerged as key regulators that can guide epigenetic modifiers like DNMT1 to specific genomic loci (23). Building on this paradigm and the aforementioned established associations, the present study hypothesized that the lncRNA LINC00184 functions as an oncogenic driver in ESCC by recruiting DNMT1 to the NDRG2 promoter, inducing its hypermethylation and transcriptional silencing. The consequent loss of NDRG2 would then relieve the brake on the PI3K/AKT pathway, leading to its sustained activation and ultimately promoting tumor cell proliferation and survival.

The present study systematically dissected the oncogenic circuitry of LINC00184 in ESCC by integrating gain- and loss-of-function analyses with pharmacological inhibition of DNMT1. Specifically, the present study investigated how LINC00184-directed, DNMT1-dependent hypermethylation of the NDRG2 promoter governs proliferative capacity, apoptotic threshold and migratory potential of esophageal squamous carcinoma cells. Furthermore, the present study employed 5-azacytidine (5-AZA), a clinically approved DNMT1 inhibitor-to evaluate the reversibility of LINC00184-evoked epigenetic silencing and to validate the therapeutic tractability of the LINC00184-DNMT1-NDRG2 axis. These data will not only refine current mechanistic understanding of ESCC biology but will also provide pre-clinical evidence for repositioning DNMT1 inhibitors in precision oncology of esophageal cancer.

Materials and methods

Cell lines and cell culture. ESCC lines KYSE-150 and TE-1 were obtained from the Cell Bank of the Chinese Academy of Sciences. KYSE-150 is one of the most classic and extensively used cell lines in ESCC research, with a well-defined ESCC origin and characteristics. TE-1 is another well-characterized and commonly utilized ESCC cell line. KYSE-150 cultures were maintained in a 1:1 mixture of RPMI-1640 and Ham's F-12 basal media supplemented with 10% (v/v) fetal bovine serum (FBS) and 1% (v/v) penicillin-streptomycin. TE-1 cultures were grown in RPMI-1640 containing identical supplements. Cells were incubated at 37˚C under a humidified atmosphere containing 5% CO_2 and routinely tested for mycoplasma contamination (negative).

Plasmid construction and transfection. For ectopic expression, the full-length LINC00184 sequence (gene ID, 100302691; National Center for Biotechnology Information) was gene-synthesized and inserted into the pLVX-mCMV-ZsGreen-IRES-Puro lentiviral backbone (Wuhan Viraltherapy Technologies, Co., Ltd.) using conventional restriction-enzyme-based cloning. Nucleic acid constructs were used at a standardized concentration of 2 μg per well for 6-well plate transfection. For transient transfection, logarithmically growing cells were plated at $4x10^5$ cells per well in 6-well plates and transfected with either OE-LINC00184 or empty vector controls (OE-NC) using Lipofectamine® 3000 (Thermo Fisher Scientific, Inc.) according to the manufacturer's protocol. Transfection was performed at 37˚C for a continuous incubation duration of 48 h under routine cell culture conditions. Total RNA was isolated 48 h post-transfection and LINC00184 overexpression was verified by reverse transcription-quantitative PCR (RT-qPCR) using the primers detailed in Table I. Specifically, total RNA was extracted from transfected cell samples using RNAiso Plus (Takara Bio) as the RNA extraction reagent. Reverse transcription was performed with the PrimeScript™ RT Reagent Kit (Takara Bio), following the manufacturer's recommended temperature protocols. The cDNA acquired from reverse-transcribed total RNA served as the DNA template for subsequent qPCR analysis. qPCR was conducted using BeyoFast™ SYBR Green qPCR Mix (Beyotime Biotechnology). GAPDH was applied as the internal reference gene. Standard thermocycling conditions were set as initial denaturation at 95˚C for 30 sec followed by 40 cycles of 95˚C for 5 sec and 60˚C for 30 sec. Relative gene expression levels were calculated using the $2^{-\Delta\Delta Cq}$ method (24). For ectopic expression of NDRG2, the full-length human NDRG2 coding sequence (gene ID, 57447) was synthesized and cloned into the identical lentiviral backbone, generating the overexpression plasmid designated OE-NDRG2. For transient rescue experiments, cells were co-transfected with the specified combinations of OE-LINC00184, OE-NDRG2 or their respective OE-NC using Lipofectamine® 3000. Successful ectopic expression of NDRG2 was validated at translational levels by western blotting analysis.

Knockdown of LINC00184 and DNMT1 by small interfering RNA (siRNA) transfection. In total, three siRNA duplexes targeting distinct regions of LINC00184 (sequences listed in Table II) were chemically synthesized by Sangon Biotech Co., Ltd. KYSE-150 and TE-1 cells were transfected in 6-well plates using Lipofectamine® RNAiMAX (Thermo Fisher Scientific, Inc.). All siRNA transfections were performed at 37˚C following the manufacturer's standard protocol, with a final siRNA concentration of 50 nM. The random non-coding siRNA sequence described below served as the negative control for mouse DNMT1 siRNA interference. Gene silencing efficiency was detected 48 h after transfection, and all subsequent functional experiments were performed at the same

Table I. Primer sequences.

Gene	Primer sequence (5'-3')	Size, bp
Homo GAPDH	F: TCAAGAAGGTGGTGAAGCAGG	115
	R: TCAAAGGTGGAGGAGTGGGT	
Homo LINC00184	F: CCAATGAGCAGGGACTATGAT	145
	R: GCAGAGAGGCAGGAAGGTTTA	

F, forward; R, reverse.

Table II. Sequences of siRNA for LINC00184.

siRNA	Sequences (5'-3')
siLINC00184-1	S: GCAAGGCAUCACACAGAAUTT
	AS: AUUCUGUGUGAUGCCUUGCTT
siLINC00184-2	S: GGAAGAGACAUAAGGAGAATT
	AS: UUCUCCUUAUGUCUCUUCCTT
siLINC00184-3	S: GCCGUCAUCUACAAAGGAATT
	AS: UUCCUUUGUAGAUGACGGCTT

S, sense; AS, antisense; si/siRNA, small interfering RNA.

48 h post-transfection time point. The detection of knockdown efficiency by RT-qPCR adopted the identical reagent system, thermal cycling parameters and calculation method as aforementioned in the RT-qPCR section. siRNA #2, which produced the highest knock-down (>70% reduction) was selected for all subsequent loss-of-function assays. siRNA duplexes specifically targeting mouse DNMT1 transcript: Sense (S), 5'-GCU GGGAGAUGGCGUCAUA-3'; antisense (AS), 5'-CAGGGA GAUACCGCAGUAU-3'; or a random non-coding mRNA sequence: S, 5'-UUCUCCGAACGUGUCACGUTT-3'; AS, 5'-ACGUGACACGUUCGGAGAATT-3' were synthesized and reconstituted in 1X siRNA buffer (Sangon Biotech Co., Ltd.). The results of the knock-down efficiency are shown in Fig. S1.

Cell Counting Kit-8 (CCK-8) assay. For viability assessment, KYSE-150 and TE-1 cells were seeded at $5x10^3$ cells per well in 96-well plates, allowed to attach overnight (37˚C and 5% CO_2) and then subjected to plasmid transfection or 5-AZA treatment for 48 h. Subsequently, 10 μl of CCK-8 reagent (Dojindo Laboratories, Inc.) were added per well, incubated for 2 h at 37˚C, and absorbance at 450 nm was recorded on a SpectraMax® i3x microplate reader (Molecular Devices, LLC). To determine a functional and non-cytotoxic concentration, the present study performed a dose-optimization experiment using CCK-8 assays across a range of concentrations (0, 0.2, 2, 5, 10 and 20 μM). Based on these results (Fig. S2), the present study selected 2 μM for subsequent functional rescue experiments, as it effectively modulated the phenotype while keeping non-specific cytotoxicity low (cell viability reduction <15%).

Transwell migration assay. KYSE-150 and TE-1 cells were seeded at $5x10^5$ cells per well in 6-well plates and allowed to attach overnight (37˚C and 5% CO_2). Following plasmid transfection or 5-AZA exposure (48 h), cells were trypsinized, washed twice with PBS and resuspended in serum-free RPMI-1640 to a density of $3x10^5$ cells/ml. A 200 μl aliquot was plated into the upper compartment of 8.0 μm pore Transwell® inserts (Corning, Inc.); the lower compartment contained 600 μl complete medium (10% FBS) serving as chemoattractant. After 24 h incubation (37˚C and 5% CO_2), non-invading cells on the upper surface were gently removed with cotton swabs. Migratory cells on the underside were fixed in 4% paraformaldehyde for 15 min, stained with 0.5% (w/v) crystal violet for 20 min at room temperature, washed three times with PBS and captured under a phase-contrast microscope. Five random fields per insert were counted by two blinded investigators.

Apoptosis assay. After 48 h post-transfection or 5-AZA exposure, KYSE-150 and TE-1 cells were collected, washed three times with PBS and centrifuged. Apoptosis was then quantified using the Annexin V-FITC/propidium iodide (PI) Apoptosis Detection Kit (cat. no. C1062S; Beyotime Biotechnology). Briefly, cells were resuspended in 1X binding buffer and stained with 5 μl of FITC-conjugated Annexin V and 10 μl of PI for 15 min in the dark at room temperature, followed by the addition of 2 ml PBS. Apoptosis was evaluated using flow cytometry with a FACScan instrument (BD Biosciences) and analyzed using CellQuest™ software (version number 5.2.1; BD Biosciences). Unstained control and single-color compensation controls (FITC single-stained and PI single-stained cells) were applied to define negative thresholds and adjust spectral compensation. Firstly, intact single-cell populations were gated according to forward scatter and side scatter parameters to exclude cellular debris and aggregates. Subsequently, quadrant gating was performed on the Annexin V-FITC vs. PI dot plot to distinguish viable cells, early apoptotic cells, late apoptotic cells and necrotic cells for statistical analysis.

Methylation-specific PCR (MSP). To evaluate the methylation status of the NDRG2 promoter, the EpiTect Plus DNA Bisulfite Kit (cat. no. 59124; Qiagen GmbH) was employed. Genomic DNA was extracted from KYSE-150 and TE-1 cells using a conventional DNA isolation method (DP-34; Tiangen Biotech Co., Ltd.). The concentration and purity of extracted genomic DNA were determined via a Nanodrop spectrophotometer. After quantifying the DNA concentration, 1 μg of genomic DNA was subjected to bisulfite treatment following the

Table III. Primer sequences for NDRG2 promoter.

Promoter	Primer sequences (5'-3')	Size, bp
Homo NDRG2 M	F: AAGTTTATAGTGGTAAATTTATTCGG	103
	R: ATAAAAAACCAACTCAAACCCG	
Homo NDRG2 U	F: TGTGTAAAGTTTATAGTGGTAAATTTATTT	109
	R: ATAAAAAACCAACTCAAACCCACT	

NDRG2, N-Myc downstream regulated gene 2; F, forward; R, reverse; M, methylated; U, unmethylated.

manufacturer's protocol. Subsequently, the bisulfite-treated DNA was used as a template for PCR amplification, utilizing the primers provided in Table III. The PCR was performed under the following conditions: Initial denaturation at 95˚C for 10 min, followed by 35 cycles consisting of denaturation at 95˚C for 30 sec, annealing at 60˚C for 30 sec and extension at 72˚C for 10 sec, with a final extension step at 72˚C for 10 min. The PCR products were analyzed via agarose gel electrophoresis and visualized using an image analysis system. The PCR amplicons were then analyzed by 1% agarose gel electrophoresis and visualized using a Bio-Rad ChemiDoc Imaging System (Bio-Rad Laboratories, Inc.) to assess the methylation status.

Chromatin immunoprecipitation (ChIP). When the KYSE-150 cells reached 70-80% confluence, the ChIP assay was performed using a commercial ChIP Kit (cat. no. P2078; Beyotime Biotechnology). The cells were fixed with 1% formaldehyde for 10 min at ambient temperature to cross-link the DNA-protein complexes. Subsequently, the chromatin was fragmented by sonication to generate DNA fragments of 200-1,000 base pairs. The sheared chromatin was then subjected to immunoprecipitation overnight at 4˚C using specific antibodies: Mouse anti-DNMT1 (cat. no. ab13537; 1:100; Abcam) and a negative control mouse anti-IgG (cat. no. ab109489; 1:100; Abcam). Protein A/G agarose beads were employed to capture the antibody-bound chromatin complexes. After extensive washing to remove non-specific binding, the cross-links were reversed by incubating the samples at 65˚C overnight. The DNA was subsequently purified using phenol/chloroform extraction and ethanol precipitation. To verify the binding of DNMT1 to the NDRG2 promoter, PCR amplification was performed using primers specific to the NDRG2 promoter region. The sequences of these primers are detailed in Table IV. Fluorescent quantitative PCR was performed with the $2^{-\Delta\Delta Cq}$ calculation. The presence of PCR products indicated the successful enrichment of the NDRG2 promoter region in the immunoprecipitated samples, thereby confirming the interaction between DNMT1 and the NDRG2 promoter.

RNA-binding protein immunoprecipitation (RIP) assay. To elucidate the interaction between LINC00184 and DNMT1, RIP assay was performed in the present study using the RIP kit from EMD Millipore, following the manufacturer's instructions. KYSE-150 cells were disrupted with RIPA lysis buffer (cat. no. P0013B; Beyotime Biotechnology) for 5 min at 4˚C.

Table IV. NDRG2 promoter-specific primers.

NDRG2-promoter	Primer sequences (5'-3')	Size, bp
1	F: CAGACAGACCCCCAGTGTTC	204
	R: CGTTTCCTGTGGCTGAGACT	
2	F: AGTCTCAGCCACAGGAAACG	173
	R: GGAGGCTGGAGGAAAAAGAA	
3	F: CCAGAGACGGGACATTCAGT	197
	R: GCTGCTCAAGCCCTAGCTC	

NDRG2, N-Myc downstream regulated gene 2; F, forward; R, reverse.

After lysis, the cell lysate was centrifuged at 12,000 x g for 10 min at 4˚C to remove cell debris and insoluble impurities. A volume of 100 μl of the lysate was incubated with 50 μl protein A/G magnetic beads (MedChemExpress) conjugated with anti-DNMT1 antibody (cat. no. ab13537; 1:100; Abcam) or control IgG (cat. no. ab109489; 1:100; Abcam) for an extended period at 4˚C. The magnetic bead-protein complexes were subsequently isolated using a magnetic separator. The complexes were then treated with proteinase K to release the associated RNA. The purified RNA was analyzed via RT-qPCR. Total RNA extracted from the RIP samples was reverse-transcribed into cDNA using a reverse transcription kit, which was then used as the template for qPCR amplification. The qPCR system included BeyoFast™ SYBR Green qPCR Mix, specific primers targeting the target genes and cDNA template. The thermal cycling conditions were as follows: Pre-denaturation at 95˚C for 30 sec, followed by 40 cycles of denaturation at 95˚C for 5 sec and annealing/extension at 60˚C for 30 sec. Relative gene expression levels were calculated using the $2^{-\Delta\Delta Cq}$ method. The specific primers utilized in this experiment are detailed in Table I.

Western blotting. Protein lysates were obtained from KYSE-150 and TE-1 cells using a cell lysis buffer (cat. no. P0013; Beyotime Biotechnology). Protein concentrations were determined using the Bradford method and subsequently normalized. Equivalent quantities ranging from 20-40 μg of protein were resolved on 12-15% gels using SDS-PAGE and electrotransferred to PVDF membranes (MilliporeSigma). After blocking with 5% BSA for 1 h at ambient temperature,

the membranes were probed with primary antibodies overnight at 4˚C. The primary antibodies utilized were: Mouse anti-GAPDH (cat. no. 60004-1-Ig; 1:1,000; Proteintech Group, Inc.), rabbit anti-NDRG2 (cat. no. Ab174850; 1:1,000; Abcam), mouse anti-AKT (cat. no. 60203-2-Ig; 1:1,000; Proteintech Group, Inc.), rabbit anti-phosphorylated (p)-AKT (cat. no. 80455-1-RR; 1:1,000; Proteintech Group, Inc.), rabbit anti-PI3K (cat. no. 4292; 1:1,000; CST), and rabbit anti-p-PI3K (cat. no. 17366; 1:1,000; CST), anti-DNMT1 (cat. no. 5032; 1:1,000; CST). The blots were washed with TBST containing 0.1% Tween-20 at room temperature three times for 15 min per wash. The membranes were then incubated with HRP-conjugated secondary antibodies, goat anti-rabbit IgG (cat. no. A0208; 1:5,000; Proteintech Group, Inc.) and goat anti-mouse IgG (cat. no. SA00001-1; 1:5,000; Proteintech Group, Inc.) for 1 h at room temperature. Protein bands were detected using a Clarity™ Western ECL Substrate (Bio-Rad Laboratories, Inc.) and their relative intensities were assessed by Quantity One analysis tool (Bio-Rad Laboratories, Inc.).

Statistical analysis. Statistical analyses were conducted using GraphPad Prism software (version 5; Dotmatics). For pairwise comparisons, an unpaired Student's t-test was employed. In cases involving multiple treatment groups, one-way ANOVA was performed, followed by Tukey's post hoc test for multiple comparisons. All experiments in this study were performed with no fewer than three independent biological replicates and the number of experimental repeats varied appropriately according to different experimental designs. Data are presented as mean ± SEM. $P<0.05$ was considered to indicate a statistically significant difference.

Results

Overexpression of LINC00184 promotes proliferation and migration while inhibiting apoptosis in ESCC cells. In order to explore the role of LINC00184 in ESCC cell proliferation, migration and apoptosis, KYSE-150 and TE-1 cells were transfected with the OE-LINC00184 plasmid to overexpress LINC00184. The expression level of LINC00184 in KYSE-150 and TE-1 cells following transfection was verified using RT-qPCR. The results demonstrated that the expression level of LINC00184 was significantly increased after transfection with the OE-LINC00184 plasmid in KYSE-150 (Fig. 1A) and TE-1 cells (Fig. 1B). In addition, the biological behaviors of cells were assessed using CCK-8 staining, Transwell and apoptosis assays. As presented in Fig. 1C and D, overexpression of LINC00184 markedly enhanced the cell viability of these two cells. The Transwell assay results revealed the increased number of migrated cells in the OE-LINC00184 groups compared with the control groups which means that overexpression of LINC00184 significantly promoted the migration of KYSE-150 cells (Fig. 1E and F) and TE-1 cells (Fig. 1G and H). Additionally, flow cytometry analysis of apoptosis indicated that the apoptotic rates in the OE-LINC00184 groups were significantly lower compared with those in the control groups which means that overexpression of LINC00184 reduced the apoptosis rate in both KYSE-150 cells (Fig. 1I and J) and TE-1 cells (Fig. 1K and L). In summary, these findings suggested that overexpression of LINC00184 serves a key role in promoting the proliferation, migration, and inhibiting apoptosis of ESCC cells.

LINC00184 negatively regulates NDRG2 and activates the PI3K/AKT pathway in ESCC cells. To elucidate the molecular mechanisms underlying the effects of LINC00184 in ESCC cells, the present study focused on its impact on NDRG2 expression and the PI3K/AKT signaling pathway. NDRG2 is a tumor suppressor protein that inhibits cell proliferation and promotes apoptosis in various cancer types, including lung, liver and pancreatic cancer (16-18). NDRG2 can inhibit the PI3K/AKT pathway by acting as a bridge between PP2A and PTEN, leading to the dephosphorylation of phosphatidylinositol-3,4,5-triphosphate and subsequent inhibition of AKT activity (21). Due to this background, the present study hypothesized that LINC00184 might influence ESCC cell behavior by regulating NDRG2, thereby affecting the PI3K/AKT pathway. Western blotting analysis in KYSE-150 and TE-1 cells revealed that overexpression of LINC00184 significantly decreased NDRG2 protein levels (Fig. 2A, B, F and G). Consistent with this, RT-qPCR analysis confirmed that LINC00184 overexpression also led to a significant reduction in NDRG2 mRNA levels in both cell lines (Fig. 2E and J), demonstrating transcriptional downregulation. Concurrently, the overexpression increased the phosphorylation of AKT (Fig. 2A, C, F and H) and PI3K (Fig. 2A, D, F and I), indicative of PI3K/AKT pathway activation. These results suggested that LINC00184 may promote ESCC cell proliferation and survival by transcriptionally repressing NDRG2 and leading to reduced NDRG2 protein expression, thereby influencing the PI3K/AKT pathway.

Restoration of NDRG2 attenuates LINC00184-induced oncogenic phenotypes. To directly establish the causal role of NDRG2 downregulation in mediating the effects of LINC00184, the present study performed a rescue experiment by re-expressing NDRG2 in TE-1 cells stably overexpressing LINC00184. Western blotting analysis confirmed the successful restoration of NDRG2 protein (Figs. 3A and S3A). Notably, this restoration significantly reversed the LINC00184-induced hyperphosphorylation of AKT (Figs. 3A and S3B), indicating that NDRG2 reconstitution effectively suppressed the activation of the PI3K/AKT pathway. Correspondingly, functional assays demonstrated that re-expression of NDRG2 significantly attenuated the enhanced cell viability promoted by LINC00184 overexpression (Fig. 3B). Collectively, these data provided direct genetic evidence that the downregulation of NDRG2 is a pivotal and causative event through which LINC00184 activates the PI3K/AKT pathway and drives proliferative advantage in ESCC cells.

LINC00184 regulates NDRG2 expression through DNMT1-mediated methylation of the NDRG2 promoter. To elucidate the regulatory mechanisms of LINC00184 on NDRG2 expression in ESCC cells, the present study first validated the effects of both LINC00184 overexpression and knockdown using siRNA (Fig. 4A and B). The present study identified that overexpression of LINC00184 markedly increased the methylation level of the NDRG2 promoter, as confirmed by MSP assay (Fig. 4C and D). By contrast, silencing

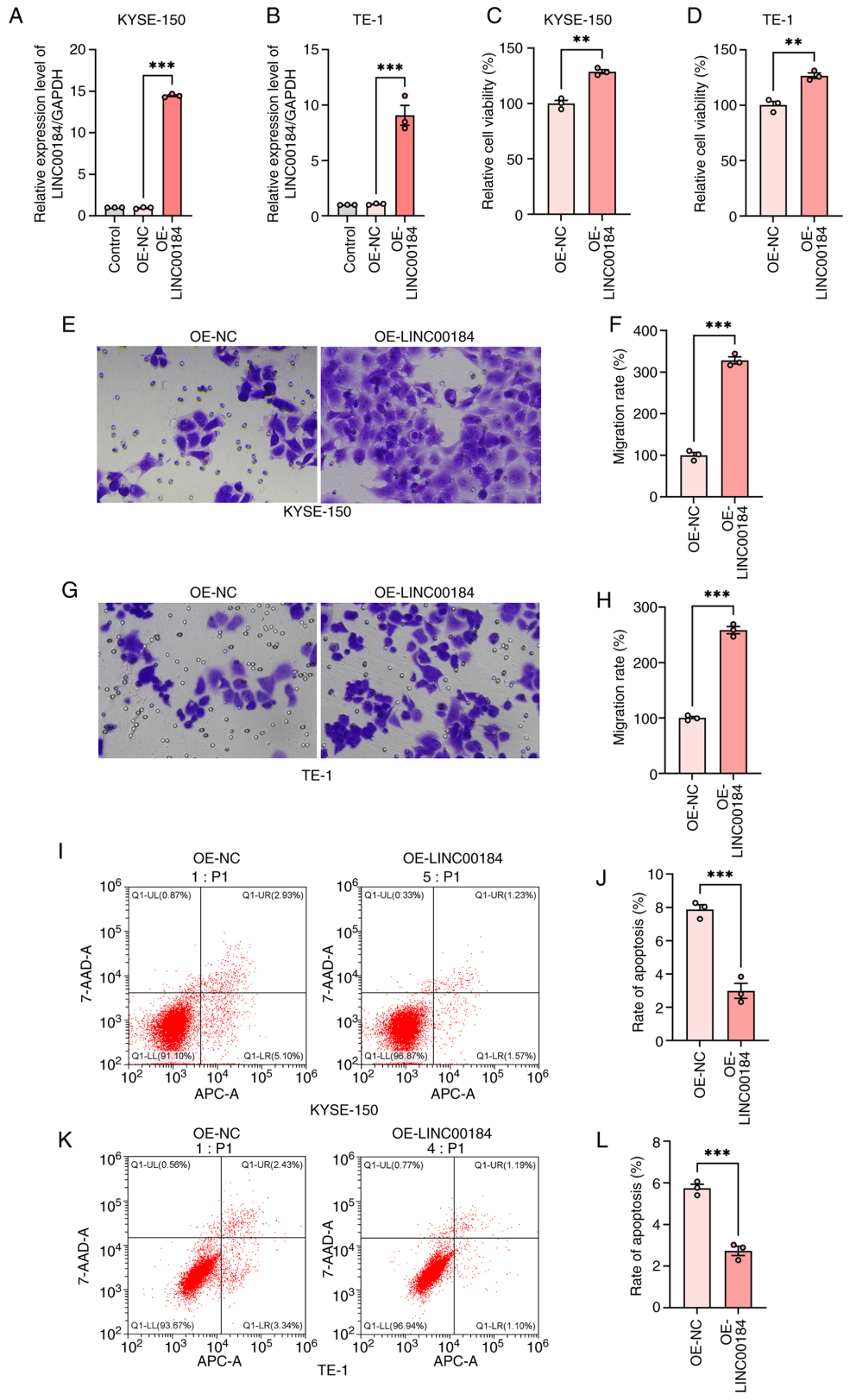

Figure 1. Overexpression of LINC00184 promotes proliferation and migration while inhibiting apoptosis in esophageal squamous cell carcinoma cells. (A) Expression level of LINC00184 in KYSE-150 cells following transfection with OE-NC and OE-LINC00184 plasmids. (B) Expression level of LINC00184 in TE-1 cells following transfection with OE-NC and OE-LINC00184 plasmids. (C) Relative cell viability in KYSE-150 cells following transfection with OE-NC and OE-LINC00184 plasmids. (D) Relative cell viability in TE-1 cells following transfection with OE-NC and OE-LINC00184 plasmids. (E) Representative images of migrated KYSE-150 cells after transfection with OE-NC and OE-LINC00184 (magnification, x200). (F) Quantitative analysis of migrated cell numbers corresponding to (E). (G) Representative images of migrated TE-1 cells after transfection with OE-NC and OE-LINC00184 (magnification, x200). (H) Quantitative analysis of migrated cell numbers corresponding to (G). (I) Flow cytometry dot plots showing the apoptosis rate of KYSE-150 cells in the OE-NC and OE-LINC00184 groups. (J) Quantitative analysis of apoptosis rates corresponding to (I). (K) Flow cytometry dot plots showing the apoptosis rate of TE-1 cells in the OE-NC and OE-LINC00184 groups. (L) Quantitative analysis of apoptosis rates corresponding to (K). Data are presented as mean ± SEM (n=3). Comparisons between two groups were performed using the unpaired Student's t-test. Statistical significance is indicated as **P<0.01 and ***P<0.001. OE, overexpression; NC, negative control.

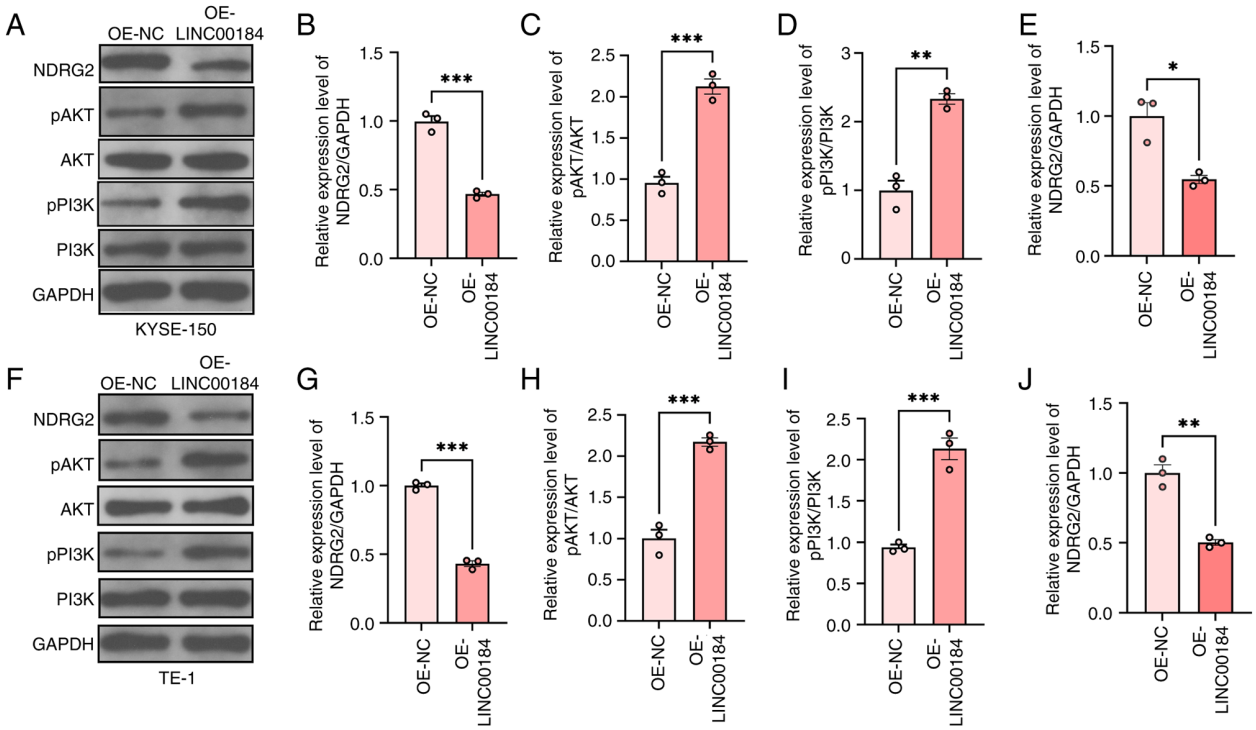

Figure 2. LINC00184 negatively regulates NDRG2 and activate the PI3K/AKT pathway in esophageal squamous cell carcinoma cells. (A) Western blotting analysis reveals the protein expression levels of NDRG2, p-AKT (Ser473), AKT, p-PI3K (Tyr458) and PI3K in KYSE-150 transfected with OE-NC or OE-LINC00184 plasmid. (B) Quantitative analysis of immunoblots of NDRG2 presented in (A). (C) Quantitative analysis of immunoblots of pAKT/AKT presented in (A). (D) Quantitative analysis of immunoblots of pPI3K/PI3K presented in (A). (E) RT-qPCR analysis of NDRG2 mRNA levels in KYSE-150 cells under control conditions and following overexpression of LINC00184. (F) Western blotting analysis demonstrating the protein expression levels of NDRG2, p-AKT (Ser473), AKT, p-PI3K (Tyr458) and PI3K in KYSE-150 and TE-1 cells transfected with OE-NC or OE-LINC00184 plasmid. (G) Quantitative analysis of immunoblots of NDRG2 presented in (F). (H) Quantitative analysis of immunoblots of pAKT/AKT presented in (F). (I) Quantitative analysis of immunoblots of pPI3K/PI3K presented in (F). (J) RT-qPCR analysis of NDRG2 mRNA levels in TE-1 cells under control conditions and following overexpression of LINC00184. Data are presented as mean ± SEM (n=3). Comparisons between two groups were performed using the Student's t-test. Statistical significance is indicated as *P<0.05, **P<0.01 and ***P<0.001. OE, overexpression; NC, negative control; RT-qPCR, reverse transcription-quantitative PCR; NDRG2, N-Myc downstream regulated gene.

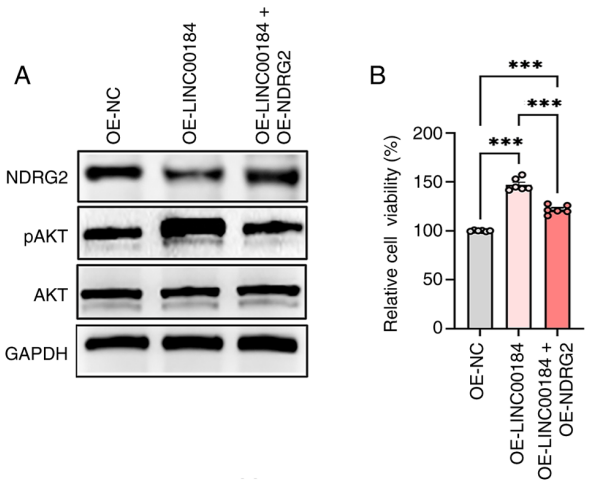

Figure 3. Restoration of NDRG2 rescues LINC00184-driven PI3K/AKT activation and proliferation in esophageal squamous cell carcinoma cells. (A) Western blotting analysis of NDRG2 and phosphorylated AKT (p-AKT) protein levels in TE-1 cells under the following conditions: Control, overexpression of LINC00184 alone (OE-LINC00184), and co-overexpression of LINC00184 and NDRG2. GAPDH serves as the loading control. (B) Cell viability measured by Cell Counting Kit-8 assay in TE-1 cells under the same treatment conditions as in (A). Data in (B) are presented as mean ± SEM (n=6). Comparisons among multiple groups were analyzed by one-way analysis of variance. ***P<0.001. OE, overexpression; NC, negative control; NDRG2, N-Myc downstream regulated gene.

LINC00184 using siRNA markedly reduced the methylation level of the NDRG2 promoter (Fig. 4C and D). These initial findings prompted further investigation into the role of DNA methylation in LINC00184-mediated NDRG2 regulation. DNMT1 is a key enzyme responsible for maintaining DNA methylation patterns, particularly during DNA replication (13). Due to its key function in epigenetic regulation, the present study hypothesized that LINC00184 might influence NDRG2 expression through DNMT1-mediated methylation of the NDRG2 promoter. To investigate this hypothesis, the present study conducted ChIP assays to examine the enrichment of DNMT1 at the NDRG2 promoter region. The results indicated that overexpression of LINC00184 led to significantly increased enrichment of DNMT1 at the NDRG2 promoter (Fig. 4E), suggesting that LINC00184 recruits DNMT1 to the NDRG2 promoter. By contrast, silencing LINC00184 using siRNA significantly decreased the enrichment of DNMT1 at the NDRG2 promoter (Fig. 4E), further supporting the role of LINC00184 in DNMT1 recruitment. To confirm the direct interaction between LINC00184 and DNMT1, the present study performed RIP assays. The results revealed that overexpression of LINC00184 significantly increased the enrichment of LINC00184 by DNMT1 (Fig. 4F and G), indicating a direct interaction between LINC00184 and DNMT1. By contrast, silencing LINC00184 significantly decreased this enrichment

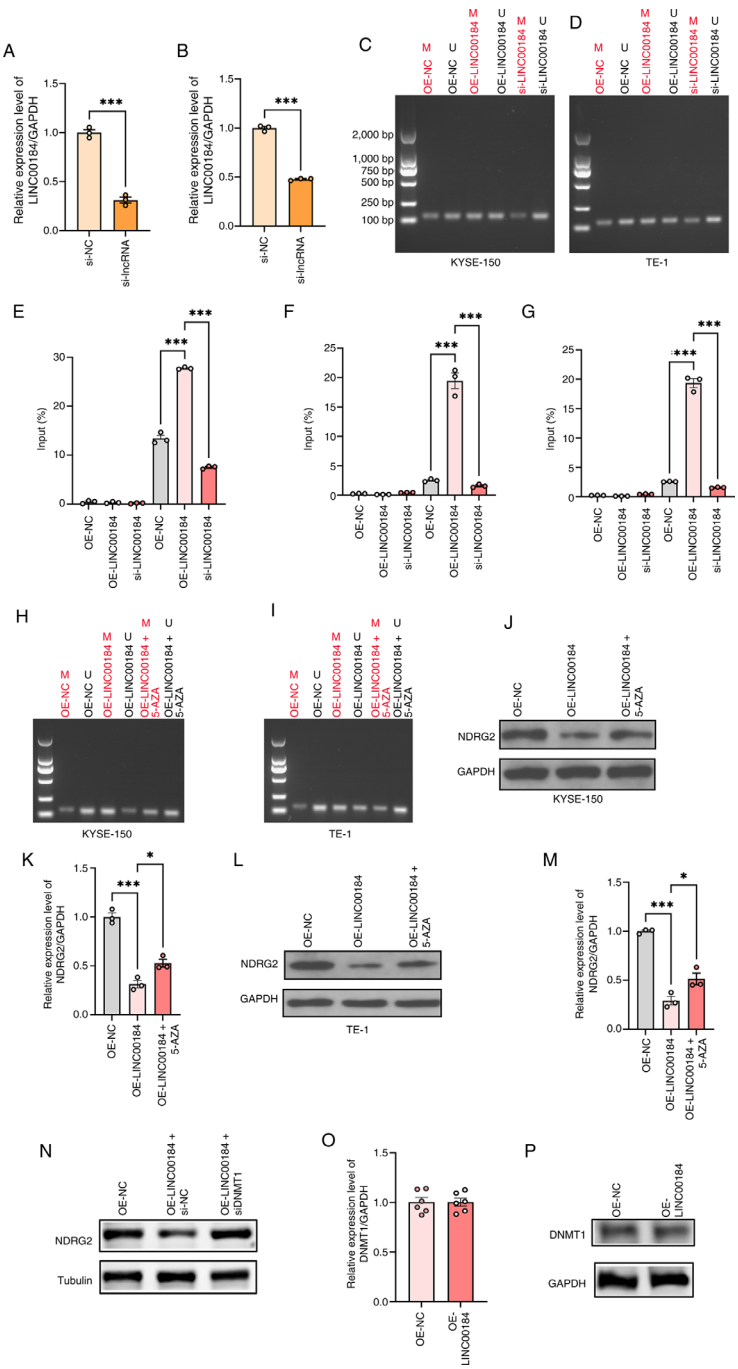

Figure 4. LINC00184 regulates NDRG2 expression through DNMT1-mediated methylation of the NDRG2 promoter. (A) Expression level of LINC00184 in KYSE-150 cells following treatment with siRNA targeting LINC00184 (n=3). (B) Expression level of LINC00184 in TE-1 cells following treatment with siRNA targeting LINC00184 (n=3). (C) Methylation level of the NDRG2 promoter in KYSE-150 cells detected via MSP assay after overexpression or silencing of LINC00184. (D) Methylation level of the NDRG2 promoter in TE-1 cells detected via MSP assay after overexpression or silencing of LINC00184. (E) Enrichment of DNMT1 at the NDRG2 promoter region detected by chromatin immunoprecipitation assay and quantified using RT-qPCR in KYSE-150 cells with overexpression or silencing of LINC00184 (n=3). (F) Enrichment of LINC00184 bound to DNMT1 detected by RNA immunoprecipitation assay and quantified using RT-qPCR in KYSE-150 cells after overexpression or silencing of LINC00184 (n=3). (G) Enrichment of LINC00184 bound to DNMT1 detected by RNA immunoprecipitation assay and quantified using RT-qPCR in TE-1 cells after overexpression or silencing of LINC00184 (n=3). (H) Methylation level of the NDRG2 promoter in KYSE-150 cells measured by MSP assay following LINC00184 overexpression combined with 5-AZA treatment. (I) Methylation level of the NDRG2 promoter in TE-1 cells measured by MSP assay following LINC00184 overexpression combined with 5-AZA treatment. (J) Western blotting analysis of NDRG2 protein expression in KYSE-150 cells after LINC00184 overexpression and 5-AZA intervention. (K) Quantitative analysis of NDRG2 protein grayscale values obtained from the western blotting results in (J) (n=3). (L) Western blotting analysis of NDRG2 protein expression in TE-150 cells after LINC00184 overexpression and 5-AZA intervention. (M) Quantitative analysis of NDRG2 protein grayscale values obtained from the western blotting results in (L) (n=3). (N) Western blotting detection of NDRG2 protein levels under control conditions, single overexpression of LINC00184, and combined treatment with OE-LINC00184 + si-DNMT1. (O) RT-qPCR detection of relative DNMT1 mRNA levels in control cells and LINC00184-overexpressing cells (n=6). (P) Western blotting analysis of total DNMT1 protein levels in control cells and LINC00184-overexpressing cells; GAPDH was used as the loading control (n=3). Data are presented as mean ± SEM (n=3). Comparisons between two groups were performed using the unpaired Student's t-test. Comparisons among multiple groups were analyzed by one-way analysis of variance. Statistical significance is indicated as *P<0.05 and ***P<0.001. OE, overexpression; NC, negative control; NDRG2, N-Myc downstream regulated gene; RT-qPCR, reverse transcription-quantitative PCR; DNMT1, DNA methyltransferase 1; si/siRNA, small interfering RNA; lnc/lncRNA, long non-coding RNA; 5-AZA, 5-azacytidine; MSP, methylation-specific PCR. M, methylation; U, unmethylation.

(Fig. 4F and G), reinforcing the notion that LINC00184 directly interacts with DNMT1. To further confirm the role of DNMT1 in LINC00184-mediated NDRG2 suppression, ESCC cells overexpressing LINC00184 were treated with the DNMT1 inhibitor 5-AZA. The results demonstrated that 5-AZA treatment effectively reversed the LINC00184-induced methylation of the NDRG2 promoter (Fig. 4H and I) and restored NDRG2 expression (Fig. 4J-M). This indicated that the methylation changes induced by LINC00184 are reversible and that DNMT1 activity is a key factor in this process. To establish a more specific causal association between DNMT1 activity and this regulatory axis, the present study employed siRNA to directly knock down DNMT1 in LINC00184-overexpressing cells. This genetic intervention successfully reversed the LINC00184-induced downregulation of NDRG2 protein (Figs. 4N and S4A), mirroring the effect observed with the pharmacological inhibitor 5-AZA. Notably, to definitively rule out the alternative possibility that LINC00184 suppresses NDRG2 by first upregulating DNMT1 expression, the present study assessed DNMT1 levels following LINC00184 manipulation. Neither DNMT1 mRNA (Fig. 4O) nor total protein levels (Figs. 4P and S4B) were significantly altered by LINC00184 overexpression. This key control experiment confirmed that LINC00184 does not affect DNMT1 abundance but instead acts by modulating the functional recruitment and activity of pre-existing DNMT1 to epigenetically silence the NDRG2 promoter. Therefore, the convergent evidence from pharmacological (5-AZA) and genetic (siDNMT1) inhibition, coupled with the unchanged DNMT1 expression profile, solidifies DNMT1 as the key epigenetic effector downstream of LINC00184.

Inhibition of DNMT1 abrogates LINC00184-induced PI3K/AKT pathway activation. Having established that LINC00184 recruits DNMT1 to silence NDRG2, the present study then investigated whether this epigenetic mechanism is responsible for the downstream activation of the oncogenic PI3K/AKT pathway. The present study first confirmed that pharmacological inhibition of DNMT1 with 5-AZA in LINC00184-overexpressing cells effectively reversed the hyperphosphorylation of both PI3K and AKT (Fig. 5A-F). To establish a specific genetic association, siRNA-mediated knockdown of DNMT1 was performed. Consistent with the pharmacological data, siDNMT1 significantly attenuated the LINC00184-induced increase in AKT phosphorylation (Fig. 5G and H). This convergence of evidence from independent inhibitory strategies definitively confirmed that the DNMT1-mediated epigenetic silencing of NDRG2 is the key mechanistic event through which LINC00184 activates the PI3K/AKT pathway in ESCC cells.

DNMT1 inhibition reverses LINC00184-induced malignant phenotypes in ESCC cells. To determine whether the DNMT1-mediated epigenetic axis is functionally required for the oncogenic phenotypes driven by LINC00184, the present study inhibited DNMT1 activity using both pharmacological and genetic approaches. Treatment of LINC00184-overexpressing cells with the DNMT1 inhibitor 5-AZA significantly reversed the pro-tumorigenic phenotypes: It significantly reduced cell viability (Fig. 6A and F), significantly attenuated enhanced cell migration (Fig. 6B, D, G and I) and significantly increased the apoptotic rate (Fig. 6C, E, H and J) back towards control levels. To provide specific genetic confirmation, siRNA-mediated knockdown of DNMT1 (siDNMT1) was performed in the same context. Consistent with the pharmacological inhibition, genetic depletion of DNMT1 also significantly reduced the enhanced cell viability induced by LINC00184 overexpression (Fig. 6K).

Collectively, these results demonstrated that DNMT1 activity is key to executing the full spectrum of the oncogenic functions of LINC00184, including promoting proliferation, migration and suppressing apoptosis. The concordance between chemical and genetic inhibition solidifies DNMT1 as a key downstream effector and a potential therapeutic target within this pathway.

Discussion

The present study revealed the significant role of LINC00184 in ESCC progression, highlighting its oncogenic function through DNMT1-mediated methylation of the NDRG2 promoter and subsequent activation of the PI3K/AKT signaling pathway. The present study results indicated that LINC00184 promotes ESCC cell proliferation and migration while inhibiting apoptosis by recruiting DNMT1 to the NDRG2 promoter, causing hypermethylation and silencing of NDRG2. This epigenetic modification activates the PI3K/AKT pathway, driving the malignant phenotype of ESCC cells. Notably, treatment with the DNMT1 inhibitor 5-AZA effectively reversed these effects, suggesting potential therapeutic strategies targeting the LINC00184/DNMT1/NDRG2 axis in ESCC.

Beyond the classical competing endogeneous RNA (ceRNA) network, LINC00184 orchestrates oncogenic signaling through multiple, context-dependent modalities. In ovarian carcinoma, it sequesters miR-1305 to relieve contactin-1 suppression and enhance tumor cell fitness (25); in gastric cancer, it competes with miR-145 for ANGPT2 mRNA, thereby driving angiogenesis and metastasis (9). Prostate cancer studies revealed that LINC00184 reduces miR-105-5p activity, leading to PD-L1 upregulation and docetaxel refractoriness (26), whereas in cholangiocarcinoma it suppresses miR-23b-3p to elevate ANXA2 and accelerate proliferation (27). In non-small cell lung cancer, the lncRNA enhances aggressiveness via the miR-524-5p/high-mobility group box 2 axis (28). The present study expands the known functional repertoire of LINC00184 by demonstrating its capacity to directly recruit the epigenetic regulator DNMT1 and facilitate DNA methylation, thereby revealing a previously unrecognized chromatin-based mechanism of action in ESCC, to the best of our knowledge.

To the best of our knowledge, the present study identified NDRG2 as a previously unrecognized downstream target whose expression is stringently controlled by LINC00184-mediated epigenetic rewriting. Although NDRG2 has been reported to be transcriptionally repressed by Myc (29), silenced by specific miRNAs (30) or modified post-translationally (31) in various malignancies. While previous studies have established the importance of NDRG2 in inhibiting tumor progression in lung (32), liver (33) and breast cancer (34), the regulatory mechanisms controlling its expression in ESCC

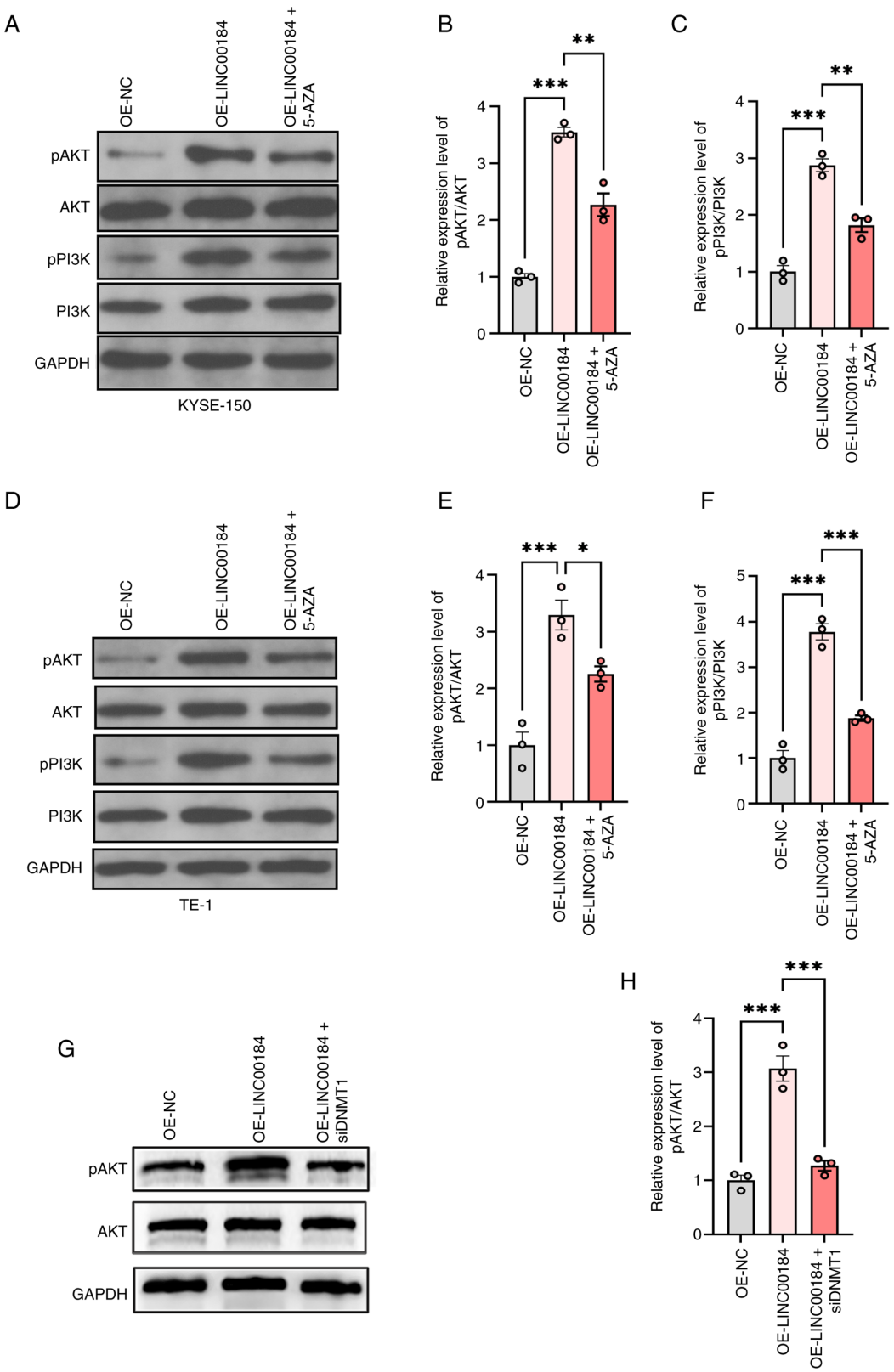

Figure 5. Inhibition of DNMT1 abrogates LINC00184-induced PI3K/AKT pathway activation and functional phenotypes. (A) Western blotting analysis showing the protein expression level of pAKT, AKT, pPI3K and PI3K in KYSE-150 cells following overexpression of LINC00184 and treatment with 5-AZA. (B) Quantitative analysis of the pAKT/AKT protein expression level derived from the immunoblots in (A). (C) Quantitative analysis of the pPI3K/PI3K protein expression level derived from the immunoblots in (A). (D) Western blotting analysis showing the protein expression level of pAKT, AKT, pPI3K and PI3K in TE-1 cells following overexpression of LINC00184 and treatment with 5-AZA. (E) Quantitative analysis of the pAKT/AKT protein expression level derived from the immunoblots in (D). (F) Quantitative analysis of the pPI3K/PI3K protein expression level derived from the immunoblots in (D). (G) Western blotting analysis of p-AKT and total AKT levels in esophageal squamous cell carcinoma cells under the following conditions: Control, OE-LINC00184 and OE-LINC00184 + si-DNMT1. (H) Quantitative analysis of the pAKT/AKT protein expression level corresponding to the immunoblots presented in (G). Data are presented as mean ± SEM (n=3). Comparisons among multiple groups were analyzed by one-way analysis of variance. Statistical significance is indicated as *P<0.05, **P<0.01 and ***P<0.001. OE, overexpression; NC, negative control; NDRG2, N-Myc downstream regulated gene; RT-qPCR, reverse transcription-quantitative PCR; DNMT1, DNA methyltransferase 1; si/siRNA, small interfering RNA; 5-AZA, 5-azacytidine.

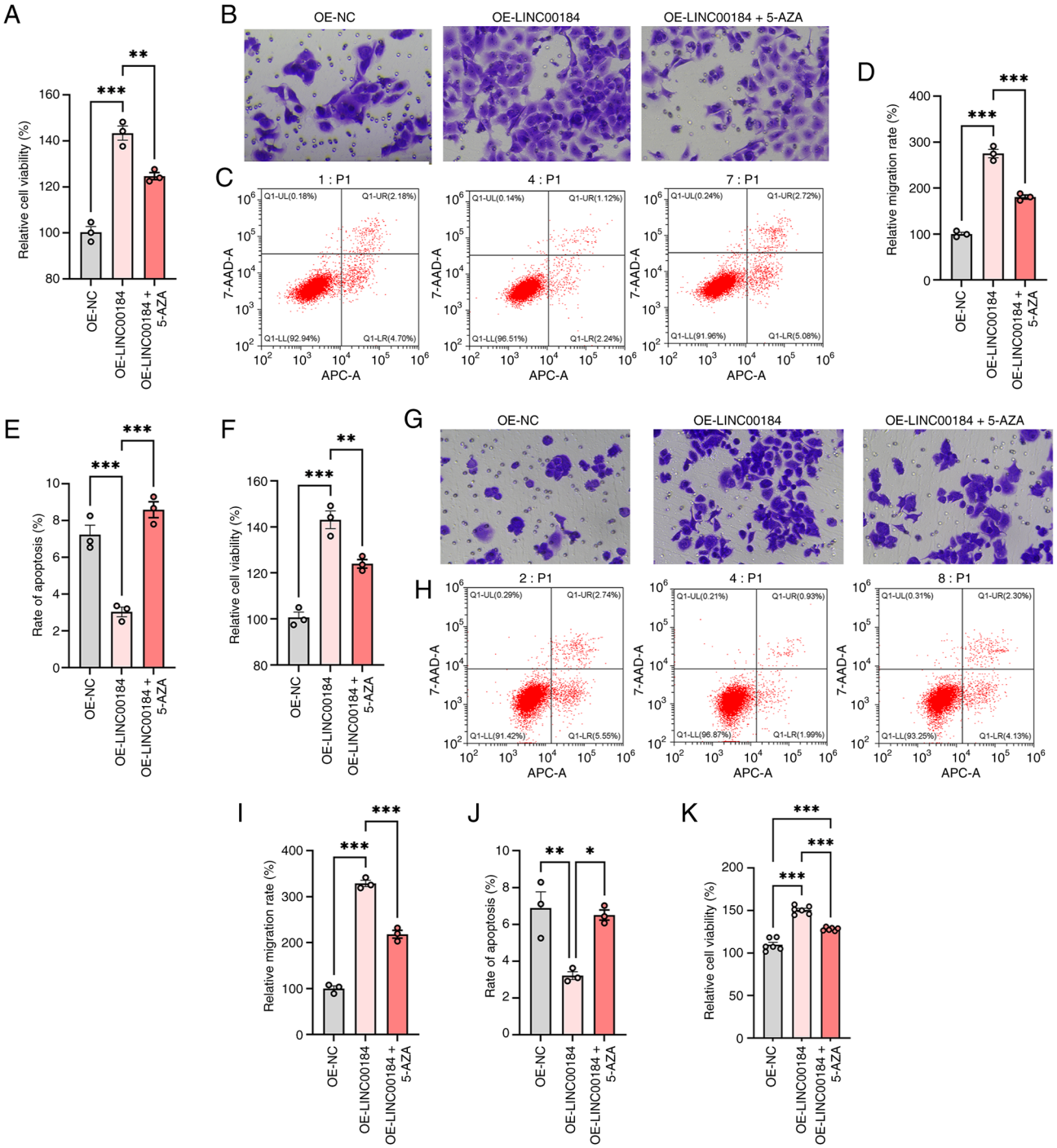

Figure 6. DNMT1 inhibition reverses LINC00184-induced malignant phenotypes in ESCC cells. (A) Cell viability of KYSE-150 cells following LINC00184 overexpression and treatment with 5-AZA (n=3). (B) Representative images of migrated KYSE-150 cells following LINC00184 overexpression and treatment with 5-AZA. (C) Representative flow cytometry dot plots showing the apoptosis rate of KYSE-150 cells following LINC00184 overexpression and treatment with 5-AZA. (D) Statistical counting of migrated KYSE-150 cells corresponding to (B) (n=3). (E) Quantitative analysis of the apoptosis rate of KYSE-150 cells corresponding to (C) (n=3). (F) Cell viability of TE-1 cells following LINC00184 overexpression and treatment with 5-AZA (n=3). (G) Representative images of migrated TE-1 cells following LINC00184 overexpression and treatment with 5-AZA. (H) Representative flow cytometry dot plots showing the apoptosis rate of TE-1 cells following LINC00184 overexpression and treatment with 5-AZA. (I) Statistical counting of migrated TE-1 cells corresponding to (G) (n=3). (J) Quantitative analysis of the apoptosis rate of TE-1 cells corresponding to (H) (n=3). (K) Cell viability detected via Cell Counting Kit-8 assay in ESCC cells under the conditions of control, OE-LINC00184 and OE-LINC00184 + si-DNMT1. Data are presented as mean ± SEM (n=3), Comparisons among multiple groups were analyzed by one-way analysis of variance. Statistical significance is indicated as *P<0.05, **P<0.01 and ***P<0.001. OE, overexpression; NC, negative control; DNMT1, DNA methyltransferase 1; si/siRNA, small interfering RNA; 5-AZA, 5-azacytidine; ESCC, esophageal squamous cell carcinoma.

remain to be elucidated. The present study findings revealed that LINC00184 recruits DNMT1 to install CpG island hypermethylation on the NDRG2 promoter, functionally extinguishing this tumor suppressor in esophageal squamous cells. Reversal of this silencing by 5-AZA not only validates the methylation-dependent mechanism but also highlights a clinically actionable route to reactivate NDRG2 in patients with ESCC.

Beyond chromatin-level regulation, the present study revealed a functional crosstalk between LINC00184 and the PI3K/AKT cascade. NDRG2 loss-of-function triggered by LINC00184-directed methylation relieves the brake on PI3K and AKT phosphorylation, thereby amplifying pro-survival signaling in ESCC cells. Due to the well-documented role of hyperactive PI3K/AKT in driving esophageal tumorigenesis and chemoresistance (22,35,36), pharmacological restoration of NDRG2 via DNMT1 blockade offers a rational strategy to dampen this oncogenic axis. The observed attenuation of PI3K and AKT phosphorylation following 5-AZA treatment substantiates DNMT1 as a tractable target to counteract LINC00184-mediated pathway hyperactivation.

The functional reversal achieved with 5-AZA underscores the therapeutic value of intercepting the LINC00184-DNMT1 interface. While DNMT1 inhibitors have demonstrated clinical efficacy in myeloid neoplasms (37), the present study pre-clinical data now extend their utility to solid tumors, specifically ESCC. Beyond classical DNMT1 blockade, rational design of AS oligonucleotides or small-molecule disruptors that specifically interfere with LINC00184-DNMT1 complex formation could provide a precision-medicine avenue in reactivating the NDRG2-PI3K/AKT brake in ESCC.

Despite these advances, the present study had certain limitations. The experiments were conducted primarily in cell lines, and further validation in primary cells, animal models and clinical samples is warranted to confirm the relevance of the present study findings *in vivo*. Furthermore, the precise molecular mechanisms by which LINC00184 recruits DNMT1 to the NDRG2 promoter remain to be fully elucidated. Future studies are warranted to explore the broader network interactions of LINC00184 with other known tumor suppressors or oncogenic pathways, which will help to contextualize its role in cancer beyond the NDRG2 axis. Future studies could also explore whether other epigenetic modifiers or co-factors are involved in the LINC00184-DNMT1-NDRG2 regulatory axis. Additionally, while the CCK-8 and Transwell assays were performed with three independent biological replicates at standardized time points to confirm the qualitative effect of LINC00184 on ESCC cell proliferation and migration, performing multi-time-point kinetics would offer further insights into the dynamics of these processes and thus, represent a beneficial direction for future studies. Notably, the lack of formal power calculations prior to conducting statistical analyses with Student's t-test and ANOVA also represents a limitation of the present study. Furthermore, the present study utilized MSP to assess the methylation status of the NDRG2 promoter CpG islands, a standard approach in detecting promoter hypermethylation; however, the absence of bisulfite sequencing constitutes a limitation of the present study, as this method would have provided single-base resolution to characterize the methylation landscape in further detail. This higher-resolution analysis represents a valuable avenue for follow-up research to refine current understanding of NDRG2 promoter methylation patterns.

In conclusion, the present study revealed a novel oncogenic function of LINC00184 in ESCC: LINC00184 acts as a molecular guide that recruits DNMT1 to epigenetically silence the tumor suppressor NDRG2. This specific silencing event, distinct from the known ceRNA role of LINC00184 in other cancer types, subsequently relieves the brake on the PI3K/AKT pathway, a key driver of ESCC progression. Thus, to the best of our knowledge, the LINC00184/DNMT1/NDRG2 axis represents a previously unrecognized epigenetic circuit integral to ESCC pathogenesis, offering both mechanistic insight and a potential therapeutic target for this aggressive cancer in the future.

Acknowledgements

Not applicable.

Funding

The present study was supported by the Shaanxi Key Research and Development Program (grant nos. 2022SF-495 and 2024SF-YBXM-121).

Availability of data and materials

The data generated in the present study may be requested from the corresponding author.

Authors' contributions

JG conceptualized the study, analyzed experimental data, conducted validation experiments, and drafted and revised the manuscript critically. SF designed the core methodology, participated in data interpretation and revised relevant manuscript content. JL performed data analysis with software, summarized research results, and revised the analytical sections of the paper. LL optimized the experimental scheme and acquisition of data. JZ verified data authenticity and supplemented results analysis. FW was responsible for the acquisition of data, and the analysis and interpretation of data. WW organized data sorting, optimized research progress management, and contributed to data analysis, interpretation, and manuscript preparation. XC improved the methodology framework, and analysis and interpretation of data. EL supervised the whole study, acquired funding, helped with conception and design, revised the full manuscript, and took overall responsibility for the research. JL and XC confirm the authenticity of all the raw data. All authors have read and approved the final version of the manuscript.

Ethics approval and consent to participate

Not applicable.

Patient consent for publication

Not applicable.

Competing interests

The authors declare that they have no competing interests.

References

1. Abnet CC, Arnold M and Wei WQ: Epidemiology of esophageal squamous cell carcinoma. Gastroenterology 154: 360-373, 2018.

2. Uhlenhopp DJ, Then EO, Sunkara T and Gaduputi V: Epidemiology of esophageal cancer: Update in global trends, etiology and risk factors. Clin J Gastroenterol 13: 1010-1021, 2020.
3. Chang J, Zhao X, Wang Y, Liu T, Zhong C, Lao Y, Zhang S, Liao H, Bai F, Lin D and Wu C: Genomic alterations driving precancerous to cancerous lesions in esophageal cancer development. Cancer Cell 41: 2038-2050.e5, 2023.
4. Liu WJ, Zhao Y, Chen X, Miao ML and Zhang RQ: Epigenetic modifications in esophageal cancer: An evolving biomarker. Front Genet 13: 1087479, 2023.
5. Zhang L, Wang Y, Gao J, Zhou X, Huang M, Wang X and He Z: Non-coding RNA: A promising diagnostic biomarker and therapeutic target for esophageal squamous cell carcinoma (review). Oncol Lett 27: 255, 2024.
6. Karakas D and Ozpolat B: The role of LncRNAs in translation. Noncoding RNA 7: 16, 2021.
7. Herman AB, Tsitsipatis D and Gorospe M: Integrated lncRNA function upon genomic and epigenomic regulation. Mol Cell 82: 2252-2266, 2022.
8. Ferrer J and Dimitrova N: Transcription regulation by long non-coding RNAs: Mechanisms and disease relevance. Nat Rev Mol Cell Biol 25: 396-415, 2024.
9. Piao HY, Guo S, Jin H, Wang Y and Zhang J: LINC00184 involved in the regulatory network of ANGPT2 via ceRNA mediated miR-145 inhibition in gastric cancer. J Cancer 12: 2336-2350, 2021.
10. Yao Y, Zhang T, Qi L, Zhou C, Wei J, Feng F, Liu R and Sun C: Integrated analysis of co-expression and ceRNA network identifies five lncRNAs as prognostic markers for breast cancer. J Cell Mol Med 23: 8410-8419, 2019.
11. Weisenberger DJ, Lakshminarasimhan R and Liang G: The role of DNA methylation and DNA methyltransferases in cancer. Adv Exp Med Biol 1389: 317-348, 2022.
12. Zhao N, Lai C, Wang Y, Dai S and Gu H: Understanding the role of DNA methylation in colorectal cancer: Mechanisms, detection, and clinical significance. Biochim Biophys Acta Rev Cancer 1879: 189096, 2024.
13. Li Z, Li B, Yu H, Wang P, Wang W, Hou P, Li M, Chu S, Zheng J, Mao L and Bai J: DNMT1-mediated epigenetic silencing of TRAF6 promotes prostate cancer tumorigenesis and metastasis by enhancing EZH2 stability. Oncogene 41: 3991-4002, 2022.
14. Li A, Omura N, Hong SM and Goggins M: Pancreatic cancer DNMT1 expression and sensitivity to DNMT1 inhibitors. Cancer Biol Ther 9: 321-329, 2010.
15. Etoh T, Kanai Y, Ushijima S, Nakagawa T, Nakanishi Y, Sasako M, Kitano S and Hirohashi S: Increased DNA methyltransferase 1 (DNMT1) protein expression correlates significantly with poorer tumor differentiation and frequent DNA hypermethylation of multiple CpG islands in gastric cancers. Am J Pathol 164: 689-699, 2004.
16. Lee KW, Lim S and Kim KD: The function of N-Myc downstream-regulated gene 2 (NDRG2) as a negative regulator in tumor cell metastasis. Int J Mol Sci 23: 9365, 2022.
17. Li SJ, Wang WY, Li B, Chen B, Zhang B, Wang X, Chen CS, Zhao QC, Shi H and Yao L: Expression of NDRG2 in human lung cancer and its correlation with prognosis. Med Oncol 30: 421, 2013.
18. Hu XL, Liu XP, Lin SX, Deng YC, Liu N, Li X and Yao LB: NDRG2 expression and mutation in human liver and pancreatic cancers. World J Gastroenterol 10: 3518-3521, 2004.
19. Feng RB, Zhou QZ, Cheng R, Li P, Zhu ST, Min L and Zhang ST: Expression and significance of N-myc downstream regulated gene 2 in the process of esophageal squamous cell carcinogenesis. Bioengineered 13: 3275-3283, 2022.
20. Ahn CH, Kim JH, Shim HW, Shin WJ, Cho YA and Yoon HJ: Biological and prognostic significance of NDRG2 downregulation in oral squamous cell carcinoma. Oral Dis 30: 4287-4302, 2024.
21. Morishita K, Nakahata S and Ichikawa T: Pathophysiological significance of N-myc downstream-regulated gene 2 in cancer development through protein phosphatase 2A phosphorylation regulation. Cancer Sci 112: 22-30, 2021.
22. Luo Q, Du R, Liu W, Huang G, Dong Z and Li X: PI3K/Akt/mTOR signaling pathway: Role in esophageal squamous cell carcinoma, regulatory mechanisms and opportunities for targeted therapy. Front Oncol 12: 852383, 2022.
23. Huang W, Li H, Yu Q, Xiao W and Wang DO: LncRNA-mediated DNA methylation: An emerging mechanism in cancer and beyond. J Exp Clin Cancer Res 41: 100, 2022.
24. Livak KJ and Schmittgen TD: Analysis of relative gene expression data using real-time quantitative PCR and the 2(-Delta Delta C(T)) method. Methods 25: 402-408, 2001.
25. Han Y, You J, Han Y, Liu Y, Huang M, Lu X, Chen J and Zheng Y: LINC00184 promotes ovarian cancer cells proliferation and cisplatin resistance by elevating CNTN1 expression via sponging miR-1305. Onco Targets Ther 14: 2711-2726, 2021.
26. Zhang W, Xin J, Lai J and Zhang W: LncRNA LINC00184 promotes docetaxel resistance and immune escape via miR-105-5p/PD-L1 axis in prostate cancer. Immunobiology 227: 152163, 2022.
27. Sun HB, Zhang GC, Liu J and Nie CS: Long noncoding RNA LINC00184 facilitates the proliferation, metastasis, and adenine metabolism of cholangiocarcinoma via modulating hsa-miR-23b-3p/ANXA2 axis. Environ Toxicol 36: 1576-1590, 2021.
28. Wang W, Li L and Zhao L: LINC00184 plays an oncogenic role in non-small cell lung cancer via regulation of the miR-524-5p/HMGB2 axis. J Cell Mol Med 25: 9927-9938, 2021.
29. Yao L, Zhang J and Liu X: NDRG2: A Myc-repressed gene involved in cancer and cell stress. Acta Biochim Biophys Sin (Shanghai) 40: 625-635, 2008.
30. Feng L, Xie Y, Zhang H and Wu Y: Down-regulation of NDRG2 gene expression in human colorectal cancer involves promoter methylation and microRNA-650. Biochem Biophys Res Commun 406: 534-538, 2011.
31. Tantai J, Pan X and Hu D: RNF4-mediated SUMOylation is essential for NDRG2 suppression of lung adenocarcinoma. Oncotarget 7: 26837-26843, 2016.
32. Ma Z, Ma Y, Feng J, Xu Z, Cheng C, Qin J, Li S, Jiang J and Kong R: NDRG2 acts as a negative regulator of the progression of small-cell lung cancer through the modulation of the PTEN-AKT-mTOR signalling cascade. Toxicol Appl Pharmacol 485: 116915, 2024.
33. Lee DC, Kang YK, Kim WH, Jang YJ, Kim DJ, Park IY, Sohn BH, Sohn HA, Lee HG, Lim JS, *et al*: Functional and clinical evidence for NDRG2 as a candidate suppressor of liver cancer metastasis. Cancer Res 68: 4210-4220, 2008.
34. Zheng J, Liu Q, Li Y, Yang J, Ma J, Yu F, Shi H, Ren Q, Zhang R, Zhang J, *et al*: NDRG2 expression regulates CD24 and metastatic potential of breast cancer cells. Asian Pac J Cancer Prev 11: 1817-1821, 2020.
35. Liu B, Wang C, Chen P, Cheng B and Cheng Y: RACKI induces chemotherapy resistance in esophageal carcinoma by upregulating the PI3K/AKT pathway and Bcl-2 expression. Onco Targets Ther 11: 211-220, 2018.
36. Shi N, Yu H and Chen T: Inhibition of esophageal cancer growth through the suppression of PI3K/AKT/mTOR signaling pathway. Onco Targets Ther 12: 7637-7647, 2019.
37. Sigalotti L, Altomonte M, Colizzi F, Degan M, Rupolo M, Zagonel V, Pinto A, Gattei V and Maio M: 5-Aza-2'-deoxycytidine (decitabine) treatment of hematopoietic malignancies: A multimechanism therapeutic approach? Blood 101: 4644-4646, 2003.